



3 4456 0514835 5

ORNL/TM-6376

ornl

OAK
RIDGE
NATIONAL
LABORATORY



Resonance Integral Calculations for Isolated Rods Containing Oxides of ²³⁸U and ²³²Th

V. C. Baker
J. H. Marable

OPERATED BY
UNION CARBIDE CORPORATION
FOR THE UNITED STATES
DEPARTMENT OF ENERGY

OAK RIDGE NATIONAL LABORATORY
CENTRAL RESEARCH LIBRARY
CIRCULATION SECTION
4500N ROOM 175
LIBRARY LOAN COPY
DO NOT TRANSFER TO ANOTHER PERSON
If you wish someone else to see this
report, send in name with report and
the library will arrange a loan.
UCR 1983 7 9 77

Printed in the United States of America. Available from
National Technical Information Service
U.S. Department of Commerce
5285 Port Royal Road, Springfield, Virginia 22161
NTIS price codes—Printed Copy: A03; Microfiche A01

This report was prepared as an account of work sponsored by an agency of the United States Government. Neither the United States Government nor any agency thereof, nor any of their employees, makes any warranty, express or implied, or assumes any legal liability or responsibility for the accuracy, completeness, or usefulness of any information, apparatus, product, or process disclosed, or represents that its use would not infringe privately owned rights. Reference herein to any specific commercial product, process, or service by trade name, trademark, manufacturer, or otherwise, does not necessarily constitute or imply its endorsement, recommendation, or favoring by the United States Government or any agency thereof. The views and opinions of authors expressed herein do not necessarily state or reflect those of the United States Government or any agency thereof.

Contract No. W-7405 eng 26

Engineering Physics Division

**RESONANCE INTEGRAL CALCULATIONS FOR ISOLATED RODS
CONTAINING OXIDES OF ^{238}U AND ^{232}Th**

(Sponsor: J. C. Cleveland; Originator: V. C. Baker)

V. C. Baker*
J. H. Marable

Date Published - February 1980

*Computer Sciences Division

OAK RIDGE NATIONAL LABORATORY
Oak Ridge, Tennessee 37830
operated by
UNION CARBIDE CORPORATION
for the
DEPARTMENT OF ENERGY

LOCKHEED MARTIN ENERGY RESEARCH LIBRARIES



3 4456 0514835 5

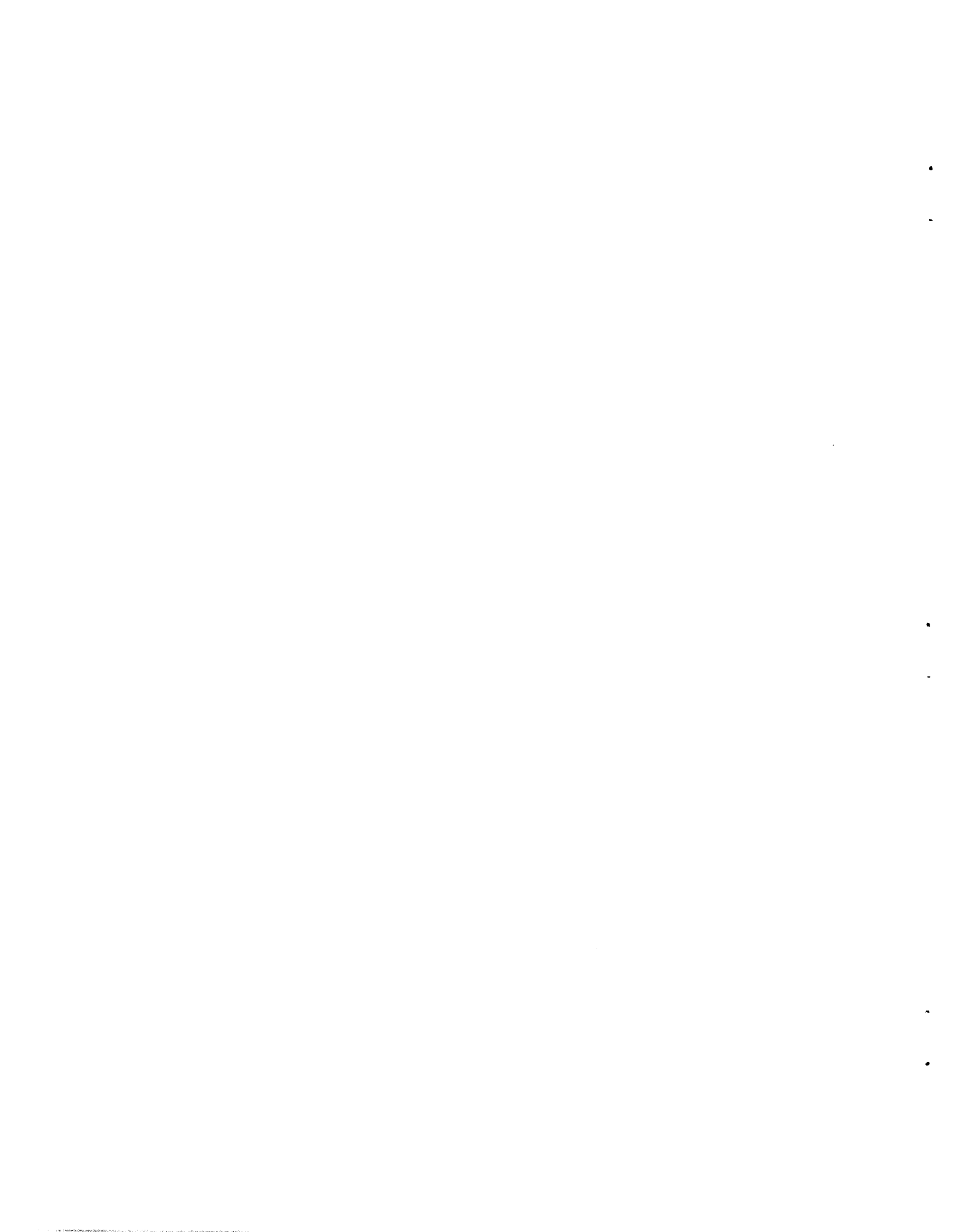
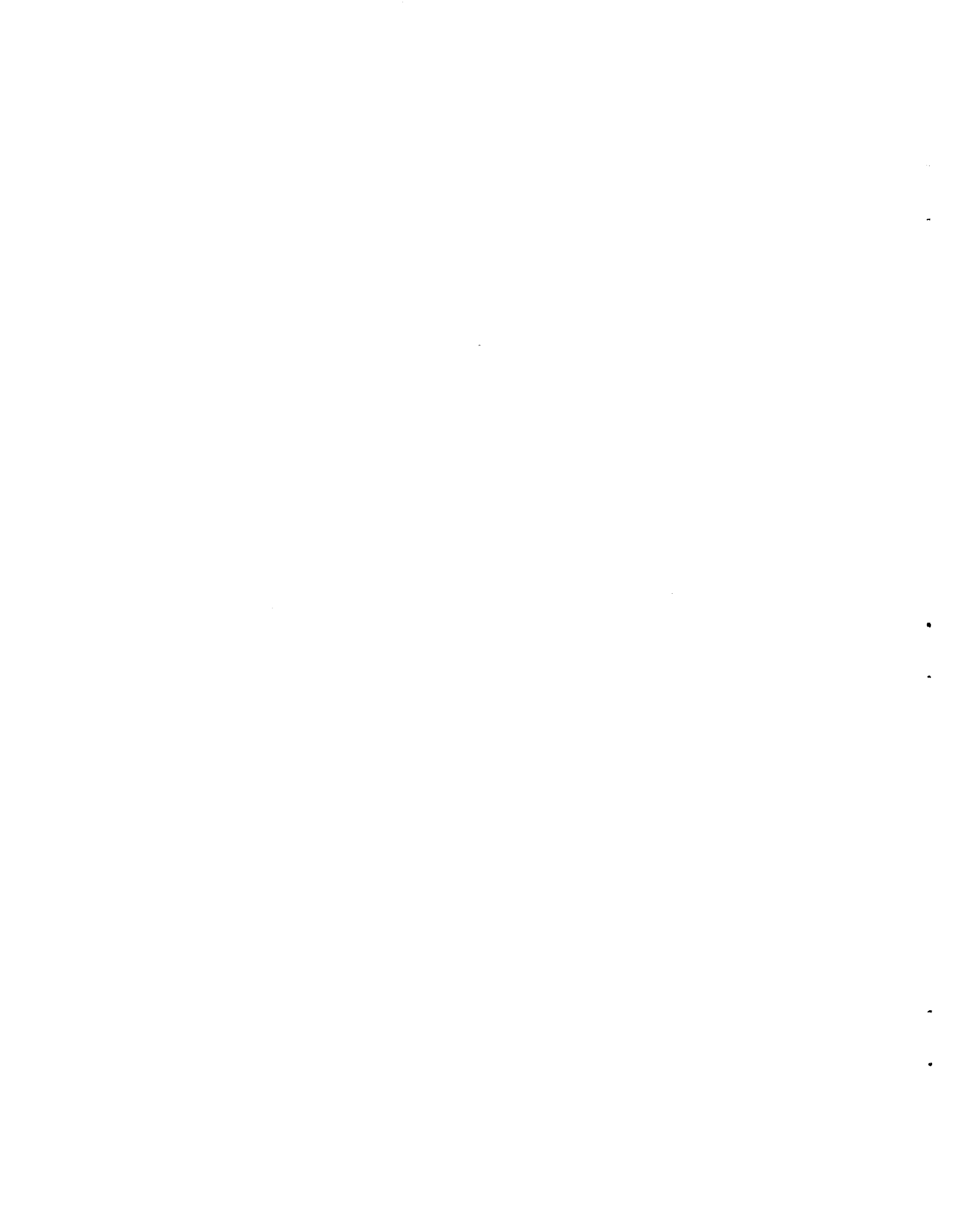


TABLE OF CONTENTS

	Page
LIST OF FIGURES	v
LIST OF TABLES	vii
ABSTRACT	1
1.0 INTRODUCTION	1
2.0 THE CALCULATIONAL METHODOLOGY	2
2.1 Definition of the Resonance Integral	2
2.2 Cross-Section Processing	4
2.3 The Transport Calculation	8
3.0 SYSTEMS ANALYZED	10
4.0 RESULTS OF THE CALCULATIONS	13
5.0 CONCLUSIONS AND RECOMMENDATIONS	24
ACKNOWLEDGMENTS	24
REFERENCES	25
Appendix A: MULTIGROUP FORM FOR THE RESONANCE INTEGRAL	27
Appendix B: SUBTRACTING OFF THE THERMAL CONTRIBUTION TO ABSORPTION	31
Appendix C: FORTRAN PROGRAM TO CALCULATE MULTIGROUP FIXED SOURCES	33



LIST OF FIGURES

	Page
2.1. Flow Diagram for Obtaining 131 Group Cross Sections from ENDF/B-IV Data	7
4.1. Resonance Integral for ^{238}U in Oxide (Case 1) (Source in Group One Only; All Cross Sections Self-Shielded for $(S/M)^{1/2} = 0.7$)	14
4.2. Resonance Integral for ^{238}U in Oxide (Case 1) (Calculated Values with Modified Source Treatment to Obtain 1/E Moderator Flux; All Cross Sections Self-Shielded for $(S/M)^{1/2} = 0.7$)	15
4.3. ^{238}U Resonance Integral UO_2 Fuel (Case 1)	17
4.4. ^{232}Th Resonance Integral ThO_2 Fuel (300°K) (Case 2)	20
4.5. ^{238}U Resonance Integral Denatured UO_2 Fuel (300°K) (Case 3)	21
4.6. ^{232}Th Resonance Integral ThO_2 Fuel (300°K) (Case 2)	22
4.7. Resonance Integral for ^{238}U in UO_2 (300°K) (Case 1)	23



LIST OF TABLES

	Page
2.1. TRX-2 131 Group Energy Boundaries	5
3.1. Resonance Integral Energy Limits	11
3.2. Fuel Rod Isotopic Compositions	11
3.3. Fuel Rod Radii and Surface-to-Mass Ratios	12
4.1. ²³⁸ U Resonance Integral UO ₂ Fuel (Case 1)	18
4.2. ²³² Th Resonance Integral ThO ₂ Fuel (Case 2)	19
4.3. ²³⁸ U Resonance Integral Denatured Urania/Thoria Fuel	19

RESONANCE INTEGRAL CALCULATIONS FOR ISOLATED RODS CONTAINING OXIDES OF ^{238}U AND ^{232}Th

V. C. Baker
J. H. Marable

ABSTRACT

This report discusses results of resonance integral calculations for UO_2 and ThO_2 isolated rods. The calculations were performed with ENDF/B-IV cross-section data and the multigroup transport code ANISN. The findings reported demonstrate by comparison to semiempirical relationships (based on experimentally derived results) the suitability of the method used for determining resonance integrals.

The calculations were based on a cylindrical rod in an H_2O moderator of large radius. Multigroup cross sections were obtained by a MINX-SPHINX-AMPX sequence, and ANISN was used to account for the neutron flux and capture rates. A special approach was used to determine a neutron source distribution such that the flux in the moderator region was forced to behave in an asymptotic way, thus providing a means by which to calculate the "ideal" resonance integral experiment.

The UO_2 resonance integrals calculated were in exceptionally good agreement with experimental values based on isolated rods. The ThO_2 results were approximately 6% lower than experimental values, and efforts to understand the discrepancy are discussed.

1.0 INTRODUCTION

During the past two decades, growing attention has been paid to the measurement and calculation of resonance integrals. In particular, contributions by Nordheim,¹ Adler,² Goodjohn and Pomraning,³ Spinard *et al.*,⁴ Rothenstein,⁵ and others have made available a wealth of documentation on the theory of neutron resonance absorption. Experiments analyzed by Hardy,⁶ Foell and Connolly,⁷ and Hellstrand^{8,9} have provided much quantitative data which has led to correlations of resonance integrals to the geometric and composition qualities of isolated heavy metal oxide fuel rods. Recently, Todosow and Carew¹⁰ have evaluated resonance integrals using ENDF/B-IV cross-section data and the multigroup cell code HAMMER.¹¹

Probably the most well-known and generally employed correlation for resonance integrals is that involving the surface-to-mass ratio (S/M) of the metal oxide of interest. The Hellstrand correlation (see Ref. 8) is widely employed in thermal reactor physics calculations and is used in a number of fuel cycle depletion codes such as LEOPARD.¹² The accuracy of Hellstrand's correlation (2-3%) has been verified only for fuel rods with relatively low S/M ($< 0.7 \text{ cm}^2/\text{gm}$ for UO_2 rods). With the advent of the denatured urania/thoria fuels, which are characterized by somewhat higher values of S/M, alternative approaches to calculating resonance integrals have been investigated. This report discusses the methodology and results obtained by a rather straightforward approach which uses evaluated neutron cross-section data (ENDF/B-IV) and discrete ordinates transport theory.

2.0 THE CALCULATIONAL METHODOLOGY

The calculational method is required to satisfy the following criteria:

1. Be amenable to calculating resonance integrals for a variety of fuel rod compositions and sizes.
2. Utilize existing computer code resources which are generally available and relatively inexpensive to use.
3. Require a minimum amount of time-consuming hand calculations.
4. Provide accuracy to within 2-3% of experimentally determined values.

These criteria have been imposed so that reliable data can be obtained at relatively low cost and with little or no requirements for new code development.

2.1 Definition of the Resonance Integral

The obvious starting point in the development of a solution procedure is to define the quantity of interest. Since the solution algorithm involves the use of multigroup transport theory, we shall derive a representation of the resonance integral in multigroup form. We begin, then, with the definition of what we mean by "resonance integral." Lamarsh¹³ has provided a quasi-physical interpretation:

. . . the resonance integral is equal to the integral of the [effective] absorption [capture] cross section over the resonance region which is necessary to account for the observed neutron absorption rate in a flux equal to that existing in the absence of the resonances.

This interpretation is quasi physical because it appears to relate a physically measurable quantity (i.e., neutron absorption rate) to some as yet undefined "effective" absorption cross section. Indeed, the resonance integral is useful for that very reason; physically measurable quantities can be *calculated* for a given fuel system in terms of its resonance integral.

We consider an isolated UO₂ fuel rod imbedded in an infinite sea of moderator. The neutron absorption rate in the ²³⁸U is

$$R = \int_{\text{Res}} {}^{238}\sigma_{\gamma}(u)\bar{\phi}_r(u)du \quad (1)$$

where u is the lethargy variable, $\phi_r(u)$ is the spatial average flux per unit lethargy in the fuel, and $\sigma_{\gamma}(u)$ is the absorption (or capture) cross section for ²³⁸U. Note that we are determining a capture rate per ²³⁸U nucleus, not absorption per unit volume; hence the use of the microscopic cross section. Of course, the flux $\phi_r(u)$ varies with lethargy since depressions appear corresponding to the ²³⁸U cross-section resonances.

We now consider some "effective cross section," $^{28}\sigma_{\text{eff}}(u)$ which would give rise to the same absorption rate, R , were the flux *not* depressed by the ^{238}U cross-section resonances. This, of course, is a hypothetical condition; nevertheless, we shall make use of the concept. In fact, let us put it another way. Suppose a uniform asymptotic (I/E) flux exists in the moderator, and a fuel rod is inserted into the flux field such that the neutron flux remains unperturbed. Obviously, if this were the case, the ^{238}U cross section must be adjusted somehow in order for the reaction rate in our hypothetical situation to be equal to that in the "real world" case. This "adjusted" cross section we shall refer to as $^{28}\sigma_{\text{eff}}(u)$. Then, in the absence of resonances, and in an asymptotic flux, the absorption rate would be

$$R = \int_{\text{Res}} ^{28}\sigma_{\text{eff}}(u)\bar{\phi}_{\text{as}} du \quad . \quad (2)$$

Equating (1) and (2) gives

$$\int_{\text{Res}} ^{28}\sigma_{\gamma}(u)\bar{\phi}_r(u) du = \int_{\text{Res}} ^{28}\sigma_{\text{eff}}(u)\bar{\phi}_{\text{as}} du \quad . \quad (3)$$

Since the asymptotic flux is constant with lethargy, we can divide both sides of Eq. (3) by ϕ_{as} to obtain

$$\frac{\int_{\text{Res}} ^{28}\sigma_{\gamma}(u)\bar{\phi}_r(u) du}{\bar{\phi}_{\text{as}}} = \int_{\text{Res}} ^{28}\sigma_{\text{eff}}(u) du \quad . \quad (4)$$

Indeed, the right-hand side of Eq. (4) is the Lamarsh definition of the resonance integral. Hence,

$$^{28}\text{R. I.} = \frac{1}{\bar{\phi}_{\text{as}}} \int_{\text{Res}} ^{28}\sigma_{\gamma}(u)\bar{\phi}_r(u) du \quad . \quad (5)$$

In terms of multigroup fluxes and cross sections, it is shown in Appendix A that Eq. (5) can be written as

$${}^2\text{8R.I.} = \frac{V_{\text{mod}}}{V_{\text{fuel}}} \left[\frac{\sum_i \sum_g V_i \sigma_{\gamma, i, g} \phi_{i, g}}{\sum_j \left(\sum_g V_j \phi_{j, g} \right) \frac{1}{\Delta U}} \right] \quad (6)$$

where g denotes energy group, V_{mod} and V_{fuel} are the total volumes of the moderator and fuel, respectively; and V_i and V_j are the interval volumes in the fuel and moderator corresponding to the multigroup fluxes $\phi_{i, g}$ and $\phi_{j, g}$, respectively. ΔU is the lethargy width corresponding to the groups over which the asymptotic flux is summed.

Implicit in the definition of the resonance integral as derived above is the assumption that the flux in the moderator behaves as $1/E$ or constant with lethargy. (Recall that it was further assumed that this flux shape would exist in the fuel were it not for resonance absorption.) It will be shown later that the requirements for an asymptotic flux behavior in the moderator play an important part in the neutron source determination for the transport calculation.

2.2 Cross-Section Processing

Multigroup cross sections used in the analysis were generated by a MINX¹⁴ – SPHINX¹⁵ – AMPX¹⁶ procedure which utilized Tomlinson's TRX-II¹⁷ 131 group structure which is shown in Table 2.1. Fig. 2.1 is a flowchart showing the basic ENDF/B-IV data files, the various processing codes, and eventually the production of an ANISN¹⁸ nuclide library.

MINX is a multigroup cross-section processing code which reads the ENDF/B file and produces pointwise and multigroup data. The MINX output data includes group averaged infinitely dilute (AMPX multigroup files) and Doppler-broadened cross sections, self-shielding factors, and group-to-group transfer matrices. The group constants produced from the TRX-II 131 group structure were calculated by using a $1/E$ spectral weighting function between .625 eV and 67 KeV and a fission spectrum between 67 KeV and 10 MeV at a fission temperature of 1.27 MeV. A Maxwellian distribution about a temperature of .02585 eV was employed for the single thermal group spanning 10^{-5} eV to .625 eV. (Actually, for the resonance integral calculation, contributions in the thermal group were not included in the total capture rates since the lower energy cutoff is about .5 eV. Consequently, the fact that MINX does not account for upscatter at thermal energies was not a problem. Details on the treatment of the low energy cutoff are given in Appendix B.)

A Bondarenko¹⁹ scheme is employed by MINX to construct table sets which account for temperature and dilution effects. Specific temperatures used were 0°K, 300°K, 900°K and 2100°K. Background cross sections ranging from 1.0 to 10^5 barns were used to construct the self-shielding tables. The temperature and self-shielding effects are quantized by F-factors which are the ratios of self-shielded and Doppler-broadened cross sections to the infinitely dilute cross sections at 0°K. MINX outputs the F-factors in standard CCCC III interface formats.

Table 2.1. TRX-2 131 Group Energy Boundaries

Group	Upper Energy (eV)	Group	Upper Energy (eV)
1	1.00000+7	36	6.79800+1
2	6.06531+6	37	6.75000+1
3	3.67879+6	38	6.68700+1
4	2.23130+6	39	6.65900+1
5	1.35335+6	40	6.63800+1
6	8.20850+5	41	6.62200+1
7	4.97871+5	42	6.61975+1
8	3.01974+5	43	6.61750+1
9	1.83156+5	44	6.61654+1
10	1.11090+5	45	6.61558+1
11	6.73795+4	46	6.61462+1
12	4.08677+4	47	6.61366+1
13	2.47875+4	48	6.61270+1
14	1.50344+4	49	6.60980+1
15	9.11882+3	50	6.60700+1
16	5.53084+3	51	6.59900+1
17	3.35463+3	52	6.58700+1
18	2.03468+3	53	6.55100+1
19	1.23410+3	54	6.52300+1
20	7.48518+2	55	6.50400+1
21	4.53999+2	56	6.46200+1
22	2.75364+2	57	6.38000+1
23	1.67017+2	58	6.32200+1
24	1.01310+2	59	5.30000+1
25	9.36000+1	60	3.97000+1
26	9.30000+1	61	3.87600+1
27	9.12800+1	62	3.81850+1
28	9.06250+1	63	3.78100+1
29	8.97500+1	64	3.75200+1
30	8.87500+1	65	3.72100+1
31	8.39200+1	66	3.69800+1
32	8.32000+1	67	3.69146+1
33	8.18000+1	68	3.68491+1
34	8.00000+1	69	3.68300+1
35	6.86800+1	70	3.68108+1

Table 2.1. (Continued)

Group	Upper Energy (eV)	Group	Upper Energy (eV)
71	3.67917+1	102	2.01500+1
72	3.67725+1	103	2.00000+1
73	3.67534+1	104	1.98000+1
74	3.66767+1	105	1.92600+1
75	3.66000+1	106	1.05000+1
76	3.65000+1	107	9.93000+0
77	3.63800+1	108	8.06000+0
78	3.60955+1	109	7.51000+0
79	3.57800+1	110	7.19000+0
80	3.54900+1	111	7.01000+0
81	3.51200+1	112	6.90000+0
82	3.46000+1	113	6.78000+0
83	2.30000+1	114	6.71000+0
84	2.24500+1	115	6.69690+0
85	2.19500+1	116	6.68387+0
86	2.15800+1	117	6.67830+0
87	2.13000+1	118	6.67280+0
88	2.11000+1	119	6.66720+0
89	2.10000+1	120	6.66170+0
90	2.09626+1	121	6.65616+0
91	2.09252+1	122	6.64310+0
92	2.09152+1	123	6.63000+0
93	2.09053+1	124	6.56000+0
94	2.08953+1	125	6.40000+0
95	2.08854+1	126	6.25000+0
96	2.08754+1	127	6.15000+0
97	2.08377+1	128	5.95000+0
98	2.08000+1	129	5.50000+0
99	2.07600+1	130	1.00000+0
100	2.06000+1	131	6.25000-1
101	2.04000+1		1.00000-5

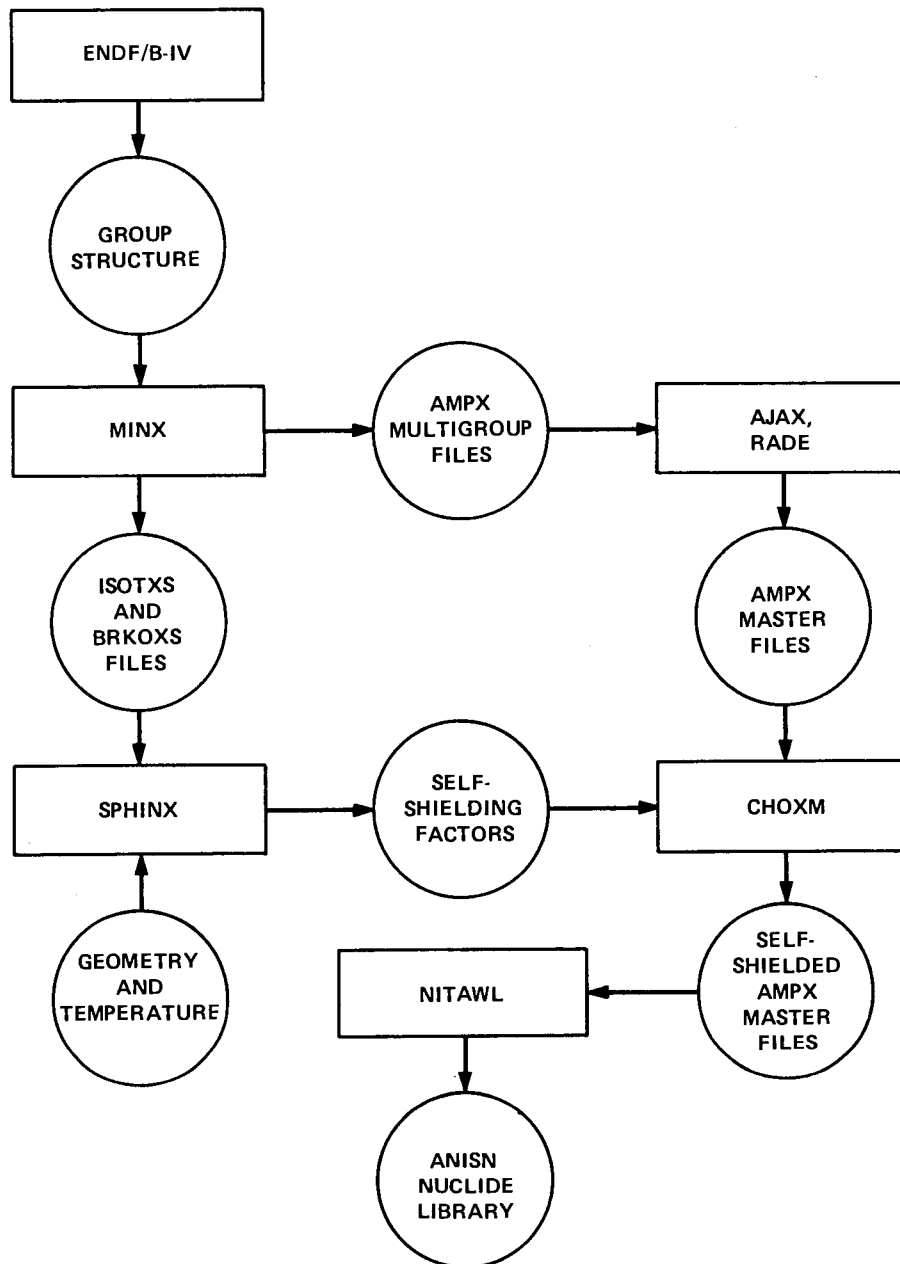


Fig. 2.1. Flow Diagram for Obtaining 131 Group Cross Sections from ENDF/B-IV Data

The SPHINX code reads two data files produced by MINX (ISOTXS and BRKOXS files) and from the geometry and composition of the fuel cell computes background cross sections for each nuclide. Fuel temperatures of 300°K and 1089°K were selected for the analysis. Using a table look-up procedure and an interpolation scheme, SPHINX generates F-factors for each nuclide at each temperature and outputs the data which is merged with the infinitely dilute AMPX master file using the CHOXM module of the AMPX system. The output from CHOXM, a self-shielded AMPX master file, is input to the NITAWL module which produces a standard nuclide library in an ANISN interface format. In order to conserve computer core requirements, each ANISN cross-section library was processed by the AXMIX²⁰ code to obtain macroscopic group independent ("GIP") libraries prior to the execution of the ANISN code.

From the SPHINX level down, the processing procedure is problem dependent; i.e., the processing for self-shielding effects and Doppler broadening must be accomplished for each ANISN run made.

2.3 The Transport Calculation

The multigroup transport code ANISN was chosen as the method by which to determine the quantities in Eq. (6), from which the resonance integral can be easily computed with a few keystrokes on a hand calculator. Recalling the correlation of S/M to resonance integrals, it was determined that holding nuclide number densities constant while varying only the fuel pin radii facilitated the process of varying S/M. Radii, corresponding number densities, and S/M for the various fuel systems investigated are tabulated in later portions of this report.

As mentioned previously, considerable attention was placed on the ability to impose an asymptotic neutron flux within the moderator. In order to determine the source distribution required, an infinite medium model and the "removal cross section" concept were employed. For an infinite, nonmultiplying medium, since there is no leakage, the neutron balance equation (assuming no upscatter) is

$$\Sigma_R(E)\phi(E) - \int_{E^+}^{E_S} \Sigma_S(E' \rightarrow E)\phi(E')dE' = S(E) \quad (7)$$

where $\Sigma_R(E)$ is the "removal cross section"

$$\Sigma_R(E) = \Sigma_T(E) - \Sigma(E \rightarrow E) \quad (8)$$

The lower limit of the integral in Eq. (7), E^+ , denotes energies just above E and the upper limit, E_s , corresponds to the source group. In multigroup form, Eq. (7) is written as

$$S_g = \Sigma_{R,g} \phi_g - \sum_{g'=g_s}^{g-1} \phi_{g'} \Sigma_s(g' \rightarrow g) \quad (9)$$

where $\Sigma_{R,g} = \Sigma_{T,g} - \Sigma_s(g \rightarrow g)$. Requiring an asymptotic flux in the moderator implies $\phi_g / \Delta U_g = \text{constant}$. Setting the constant equal to unity gives

$$\phi_g = \Delta U_g = \ln \left(\frac{E_{\text{upper}}}{E_{\text{lower}}} \right) g \quad (10)$$

for all groups.

Inserting Eq. (10) into Eq. (9) and using the multigroup cross sections for the moderator, the multigroup sources S_g can be readily generated. These sources are calculated by a simple FORTRAN program which solves Eq. (9) and punches the output in standard free-form FIDO format for use in ANISN. It was found that the multigroup fluxes per group lethargy in the moderator were quite constant when sources obtained in this fashion were used in the transport calculation. (See Appendix D for a listing of the source program used.)

In the ANISN calculation, P_0 microscopic cross sections were included as separate materials, i.e., for ^{238}U and ^{232}Th . From these were computed zonewise activities for absorption and fission rates. The capture rate is obtained by subtracting the fission rate from the absorption rate, the difference being the numerator in the square brackets in Eq. (6). This operation was done in a few seconds with the aid of a hand calculator.

The denominator in the square brackets in Eq. (6) can be rewritten as

$$\sum_j \left(\sum_g v_j \phi_{j,g} \right) \frac{1}{\Delta U} = \sum_j \frac{v_j \phi_{j,g}}{\Delta U_g} = \sum_j \frac{v_j \phi_{j,g+1}}{\Delta U_{g+1}}, \text{ etc.}, \quad (11)$$

since for an asymptotic flux $\phi_g/\Delta U_g = \text{constant} = \phi_{g+1}/\Delta U_{g+1}$, etc. To obtain this quantity directly from the ANISN output, groupwise lethargy widths were input in the 5* (velocities) array. Multigroup fluxes per unit lethargy then appear in the "density" column in the zone summary tables. Since in practice there was some slight deviation of the calculated fluxes per unit lethargy from group to group, the sum of these fluxes (also in the zonewise summary tables) was divided by the number of groups to obtain a simple average value. This operation took a few seconds using a hand calculator. All that remained to complete the solution in Eq. (6) was to multiply by the moderator to fuel volume ratio. This computation was trivial. Thus resonance integrals were computed with a minimum of hand calculations.

The ANISN calculations were run in the cylindrical geometry mode. The fuel radii varied from about 0.3 cm to about 1.0 cm, while the moderator radius was held at 10 cm for each run. A total of 30 radial intervals was used: about 12 in the fuel, 2 in the clad, and the remainder in the moderator. An S_{16} cylindrical quadrature was used, and the scattering expansion was P_3 . A white boundary condition was imposed on the outer surface of the moderator zone. Total running time from the SPHINX level through the ANISN execution was about three minutes on the IBM-360, Model 195.

3.0 SYSTEMS ANALYZED

The resonance integral sequence of calculations has been carried out for three different fuel compositions. Case 1 consists of UO_2 (~4% ^{235}U) isolated fuel rods. Cases 2 and 3 contain mixtures of uranium and thorium oxides, with Case 3 corresponding to the denatured system. Clad material used was zircalloy-2 in each case (.0635 cm thick). The energy limits for each resonance integral calculated are specified in Table 3.1. Table 3.2 gives the isotopic compositions for each case.

The UO_2 and denatured systems were analyzed at 300°K and 1089°K so that temperature effects on the resonance integral could be observed. As previously pointed out, S/M values were varied by changing the fuel radii while holding the nuclide number densities constant. Fuel radii used and the corresponding surface-to-mass ratios for the oxide indicated are given for each case in Table 3.3.

Case 1 (UO_2 fuel) was run primarily as a test case so that calculated resonance integrals could be compared with the empirical correlation of Hellstrand in order to verify the reliability of the methodology. As a check for the applicability of the group structure to calculating resonance absorption in thorium, Case 2 was run. Once the validity of the method had been tested and optimized by the first case study, the calculations for the denatured systems in Case 3 were performed. Results of the calculations are presented in the next section.

Table 3.1. Resonance Integral Energy Limits

Case	Description	E_{lower}^a	E_{upper}^b	Isotope for which R. I. Calculated
1	UO ₂ (~4% ²³⁵ U)	.625 eV	2 MeV	²³⁸ U
2	ThO ₂	.50 eV	10 MeV	²³² Th
3	Denatured (U/Th)O ₂	.55 eV	2 MeV	²³⁸ U

^aAppendix B gives a brief description of the lower energy cutoff treatment used to subtract off contributions to the resonance integral in the thermal range below the desired energy cutoff.

^bUpper energies correspond to the lowest group number which contains source neutrons.

Table 3.2. Fuel Rod Isotopic Compositions

Case	Number Densities (atoms/b-cm)				
	²³⁵ U	²³⁸ U	²³⁴ U	²³² Th	¹⁶ O
1	6.80527(-4)	2.17263(-2)	--	--	4.48136(-2)
2	8.6723 (-4)	2.1269 (-5)	4.39138(-5)	2.08748(-2)	4.36143(-2)
3	9.2909 (-4)	3.6622 (-3)	7.4220 (-6)	1.6685 (-2)	4.2568 (-2)

Table 3.3. Fuel Rod Radii and Surface-to-Mass Ratios

Case 1		Case 2		Case 3	
Radius(cm)	S/M($^{238}\text{UO}_2$, cm ² /gm)	Radius(cm)	S/M($^{232}\text{ThO}_2$, cm ² /gm)	Radius(cm)	S/M($^{238}\text{UO}_2$, cm ² /gm)
.2921	.70288	.2921	.74846	.2921	4.170
.41275	.49742	.41275	.52968	.41275	2.951
.5842	.35144	.5842	.37423	.5842	2.085
1.0160	.20208	1.0160	.21518	1.0160	1.199
--	--	--	--	1.340 ^a	0.908

^aFor this run S/M was varied by changing both the fuel rod radius and heavy metal number densities as follows:

$$N^{238}\text{U} = 1.0223(-2) \text{ atoms/b-cm}$$

$$N^{232}\text{Th} = 1.0539(-2) \text{ atoms/b-cm}$$

4.0 RESULTS OF THE CALCULATIONS

For the Case 1 study (UO₂ fuel, enriched), agreement with the Hellstrand correlation was found to be excellent once the proper source distribution and correct self-shielding treatments were imposed.* Resonance integrals calculated for ²³²Th were found to be approximately 6% lower than those measured by Hardy and Palowitch, and the reasons for these differences are unclear at this time. However, the primary suspect is the group structure used since that structure was tailored to a fine-group resolution of the ²³⁸U resonances. In spaces between the ²³⁸U resonances, the group boundary intervals are widely separated, and some of these regions correspond to the important ²³²Th resonances. Efforts to understand, explain, and ameliorate the ²³²Th integrals are under way, and the results of this investigation will be presented in some future work.

Finally, for the denatured urania/thoria system (Case 3), results appear to be favorable. Calculated resonance integrals for ²³⁸U in these systems lie between the likely limits of the Hellstrand correlation and experimental data obtained by Foell and Connolly (Ref. 7). As pointed out in Ref. 7, the Foell and Connolly fuel samples contained quantities of PbO₂ which enhance neutron scattering and result in higher resonance integrals than one would expect for systems containing no lead oxide. Moreover, the Hellstrand correlation is known to underestimate resonance integrals in UO₂ systems characterized by S/M > 0.7 cm²/gm. The tables and figures at the end of this section show the results obtained from the calculations and compare the results with various experimental and empirical data.

As noted in the footnote below, the original approach to cross-section self-shielding was to perform a single SPHINX calculation and use the resulting self-shielded cross sections for each pin cell calculated. Moreover, it was thought that by placing the source neutrons in a single high-energy group, the flux in the moderator would attain an asymptotic shape at lower energies. Figure 4.1 shows the results of the calculations using this approach compared with the Hellstrand correlation [R.I. = 5.35 + 26.6(S/M)^{1/2} barns for UO₂ fuel]. The poor agreement between the Hellstrand and calculated values is due both to the inadequacy of the self-shielding treatment and the ambiguity introduced by the single-group source in determining the asymptotic flux value.

When the source treatment was modified to impose a more nearly asymptotic flux, the results shown in Fig. 4.2 were obtained. One observes that the normalization [i.e., the constant in the linear relationship between (S/M)^{1/2} and the resonance integral] appears to have been improved by the modified source treatment, but the slope of the line appears to be incorrect. From this observation it was determined that SPHINX runs must be made for each fuel pin size to properly account for the

*Due to the fact that for different S/M values fuel rod radii were changed only slightly (fractions of a centimeter), the original approach was to use the same self-shielded cross sections obtained from SPHINX for each fuel pin of identical composition but slightly different radii. This approach proved unsuitable, however, since cross-section self-shielding was found to be rather strongly geometry (fuel rod radius) dependent. A comparison of the original and final approaches is noted in the figures.

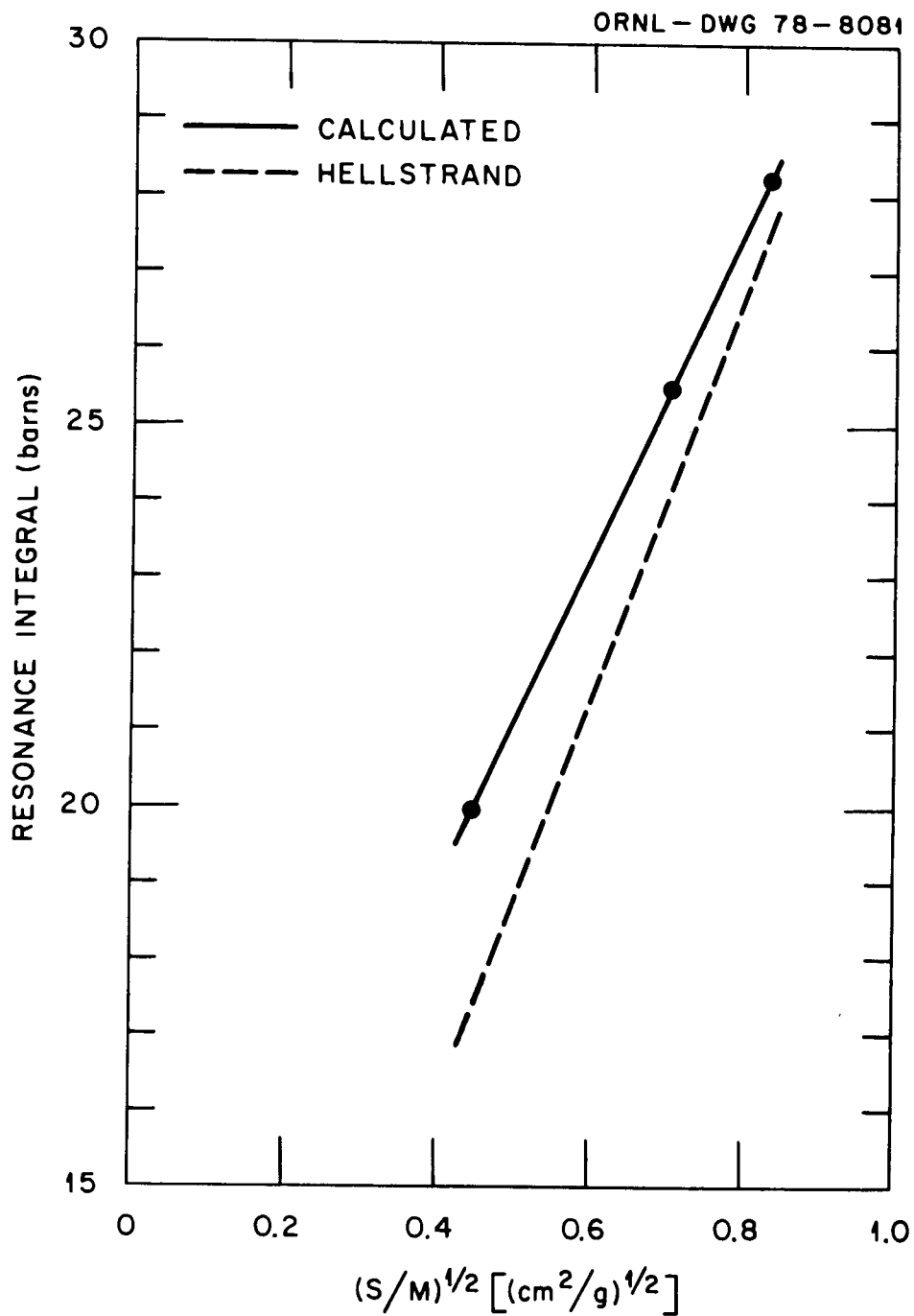


Fig. 4.1. Resonance Integral for ^{238}U in Oxide (Case 1) (Source in Group One Only; All Cross Sections Self-Shielded for $(S/M)^{1/2} = 0.7$)

ORNL - DWG 78-8082

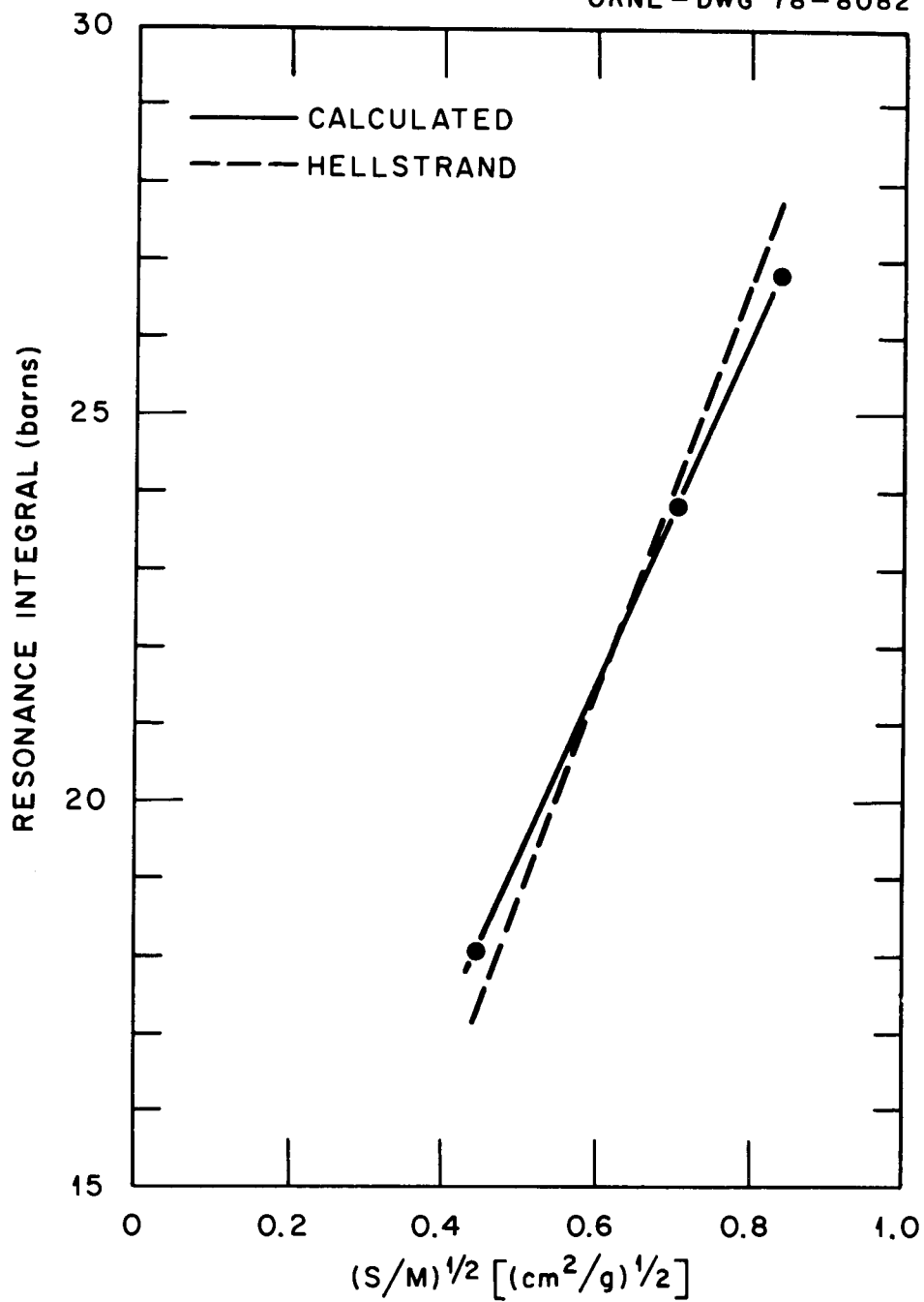


Fig. 4.2. Resonance Integral for ^{238}U in Oxide (Case 1) (Calculated Values with Modified Source Treatment to Obtain $1/E$ Moderator Flux; All Cross Sections Self-Shielded for $(S/M)^{1/2} = 0.7$)

self-shielding effects due to geometry. Figure 4.3 shows the results of the Case 1 calculation with the modified source treatment and the correct geometrical self shielding (SPHINX runs) applied for each fuel pin radius. The results show much better agreement with the Hellstrand correlation. Table 4.1 gives values for the resonance integral calculated at 300°K and 1089°K using the latter methodology, and the acceptable agreement with the Hellstrand values served to verify the adequacy of the calculational approach.

The Case 2 calculation for ^{232}Th resonance integrals in oxide fuels was performed in the latter fashion described above. The calculations reflect values roughly 6% lower than experimental values obtained by Hardy and Palowitch. Two possible sources of error are the ENDF/B-IV data and the group structure used. Recently, Ullo²¹ has inferred from an independent investigation that the ENDF/B-IV data may yield self-shielded ^{232}Th resonance integrals about 6% below those determined experimentally. Moreover, the 131 group structure used contains broad groups spanning several resolved resonances in thorium, since the group structure was explicitly created for ^{238}U resonance resolution below 100 eV. Future data testing plans call for a reanalysis of the isolated thorium oxide rods using ENDF/B-V data and a group structure more compatible with the thorium resonances. Results of the Case 2 calculations are given in Table 4.2, and Fig. 4.4 shows the comparison with the Hardy and Palowitch data.

For the denatured systems (Case 3) characterized by high S/M, resonance integrals for ^{238}U in urania/thoria systems were calculated. It is known that the Hellstrand correlation tends to underestimate resonance integrals for ^{238}U in oxide for S/M greater than about $.7 \text{ cm}^2/\text{gm}$. Experimental data obtained by Foell and Connolly for denatured systems containing urania/thoria/lead mixed oxides was expected to yield somewhat higher values for resonance integrals due to the presence of the lead oxide and the resulting increase of heavy metal scattering. Thus, the Hellstrand correlation and the Foell and Connolly experiment should provide lower and upper bounds for denatured UO_2/ThO_2 systems. Figure 4.5 shows how the calculated resonance integrals lie between these bounds, with a tendency to favor the Hellstrand correlation, especially for low values of $(\text{S}/\text{M})^{1/2}$. Further evidence that the Foell and Connolly data yields higher resonance integrals for both ^{232}Th and ^{238}U is indicated by Figs. 4.6 and 4.7. As shown by Fig. 4.6, for $(\text{S}/\text{M})^{1/2}$ greater than about .65, the Foell and Connolly thorium integrals are higher than those obtained by Hardy and Palowitch; while Fig. 4.7 shows that even for $\text{S}/\text{M} < .7 \text{ cm}^2/\text{gm}$ ($\text{S}/\text{M} < .836$), the Foell and Connolly data overestimates the Hellstrand values. In this range of S/M the Hellstrand correlation is quite accurate, and one is led to conclude that the presence of PbO_2 in the Foell and Connolly fuel samples produces the net effect of increasing the resonance integrals, especially for high S/M. This conclusion further supports the notion that the Foell and Connolly data represents an upper limit for integrals in fuel containing no PbO_2 .

ORNL-DWG 78-8083

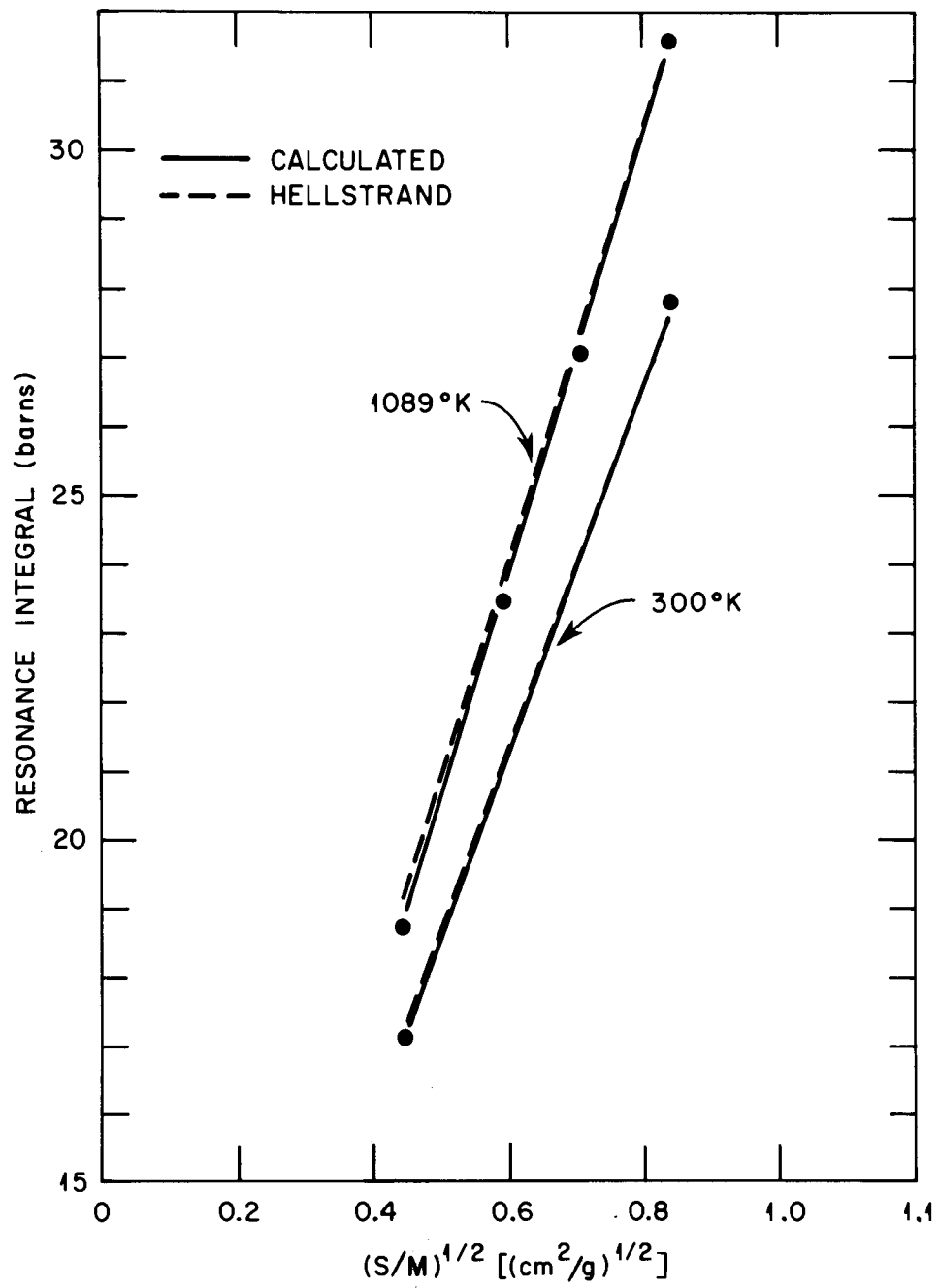
Fig. 4.3. ^{238}U Resonance Integral UO_2 Fuel (Case 1)

Table 4.1. ^{238}U Resonance Integral UO_2 Fuel (Case 1)

S/M (cm^2/gm)	Temperature	R.I. Calc. ^a (barns)	R.I. Hellstrand ^b (barns)	Calc./Hellstrand
.2021	300°K	17.12	17.31	.989
.7029	300°K	27.84	27.65	1.007
.2021	1089°K	18.75	19.15	.979
.3514	1089°K	23.39	23.62	.990
.4974	1089°K	27.09	27.24	.994
.7029	1089°K	31.61	31.69	.997

^a ENDF/B-IV cross-section data used for calculations.

^b Experimental error = 2% (Ref. 8).

Table 4.2. ^{232}Th Resonance Integral ThO_2 Fuel (Case 2)
(300°K)

S/M (cm^2/gm)	R.I. Calc. ^a (barns)	R.I. Hardy/Palowitch ^b (barns)
.2152	12.47	13.35
.3742	14.74	15.70
.5297	16.52	17.50
.7485	18.74	19.69

^a ENDF/B-IV cross-section data used in calculations.

^b Experimental uncertainty = ~ 0.6 barns for each case (Ref. 6).

Table 4.3. ^{238}U Resonance Integral Denatured Urania/Thoria Fuel

S/M (cm^2/gm)	Temperature	R.I. Calc. ^a (barns)
4.170	300°K	62.83
2.951	300°K	53.36
2.085	300°K	45.33
1.199	300°K	35.36
0.908	300°K	31.27
1.199	300°K	34.90
4.170	1089°K	77.85
2.951	1089°K	65.03
2.085	1089°K	54.39
1.199	1089°K	41.04
0.908	1089°K	35.90
1.199	1089°K	40.67

^a ENDF/B-IV cross-section data used in calculations.

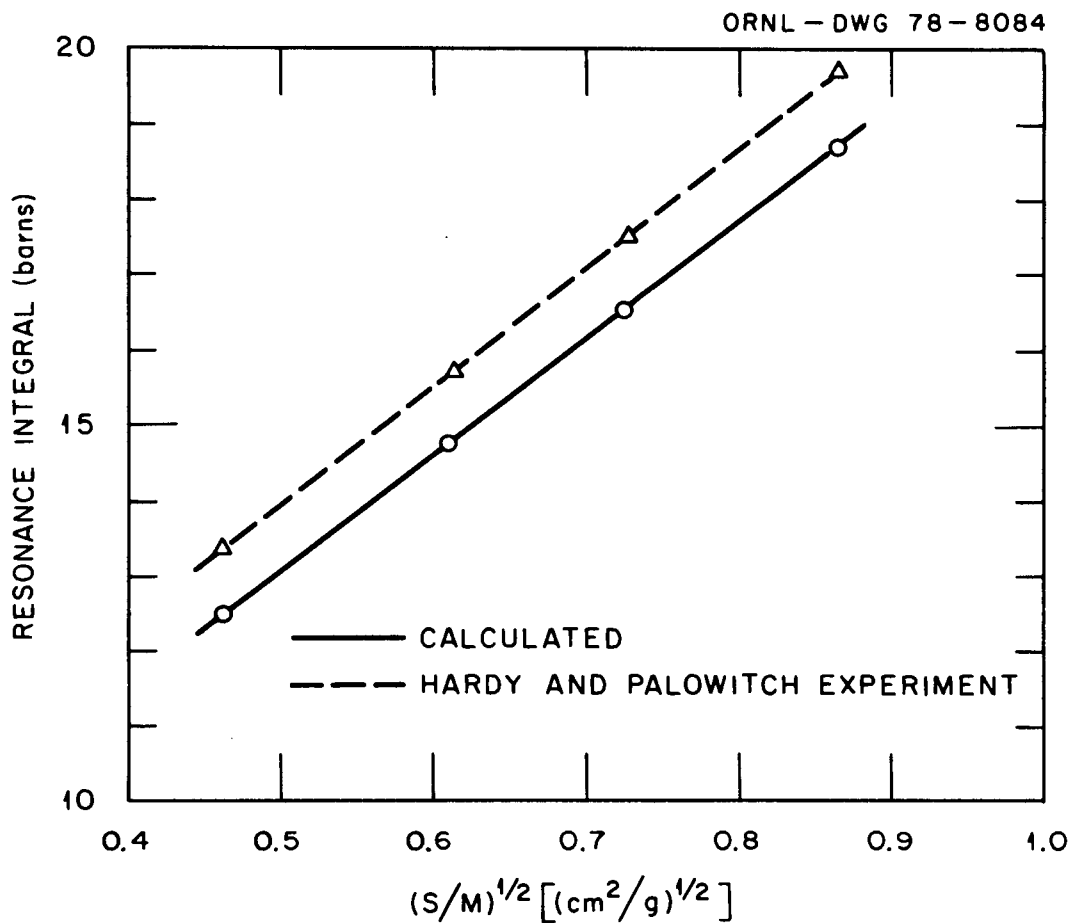


Fig. 4.4. ²³²Th Resonance Integral ThO₂ Fuel (300°K) (Case 2)

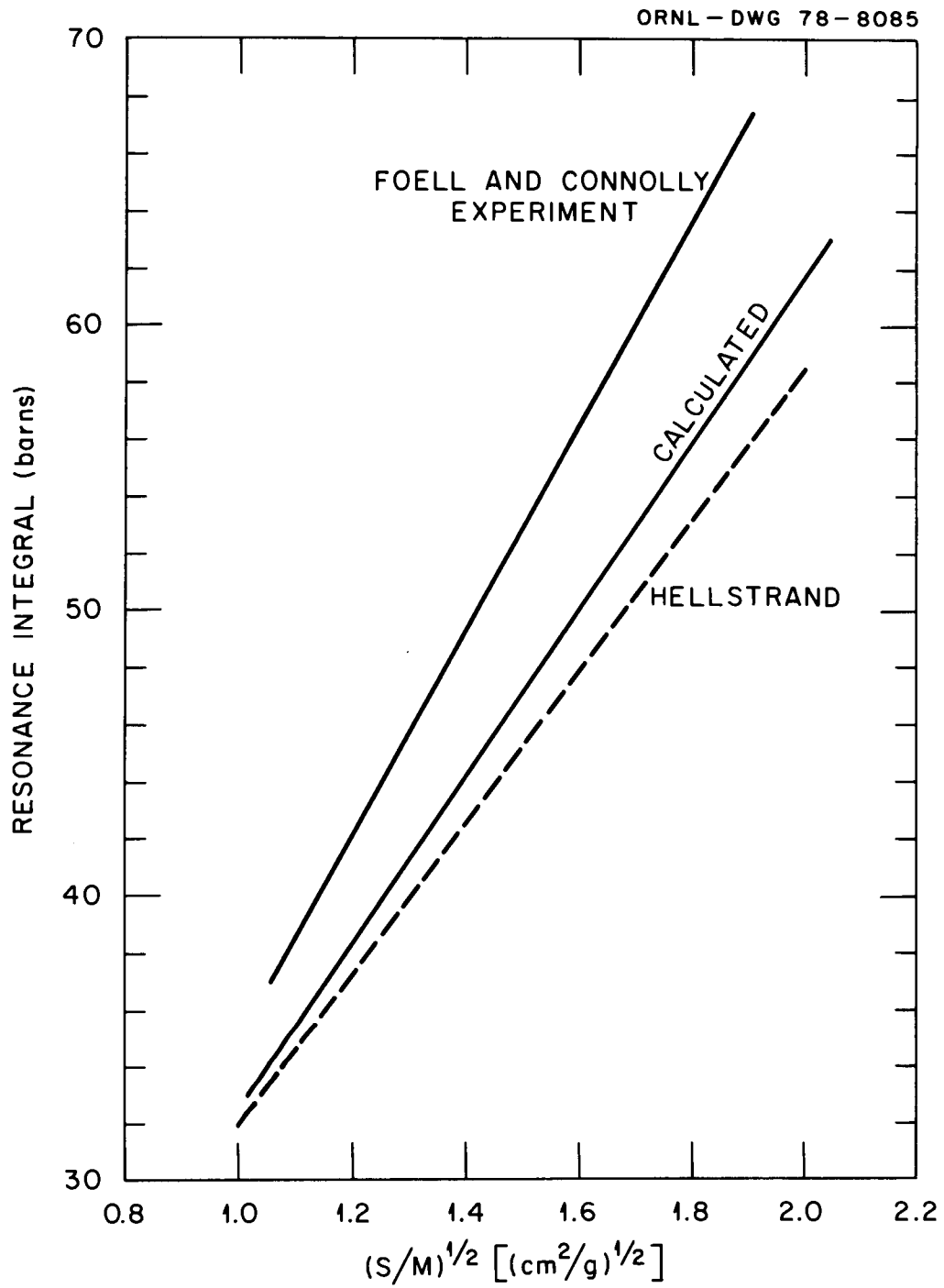


Fig. 4.5. ^{238}U Resonance Integral Denatured UO_2 Fuel (300°K) (Case 3)

ORNL-DWG 78-8086

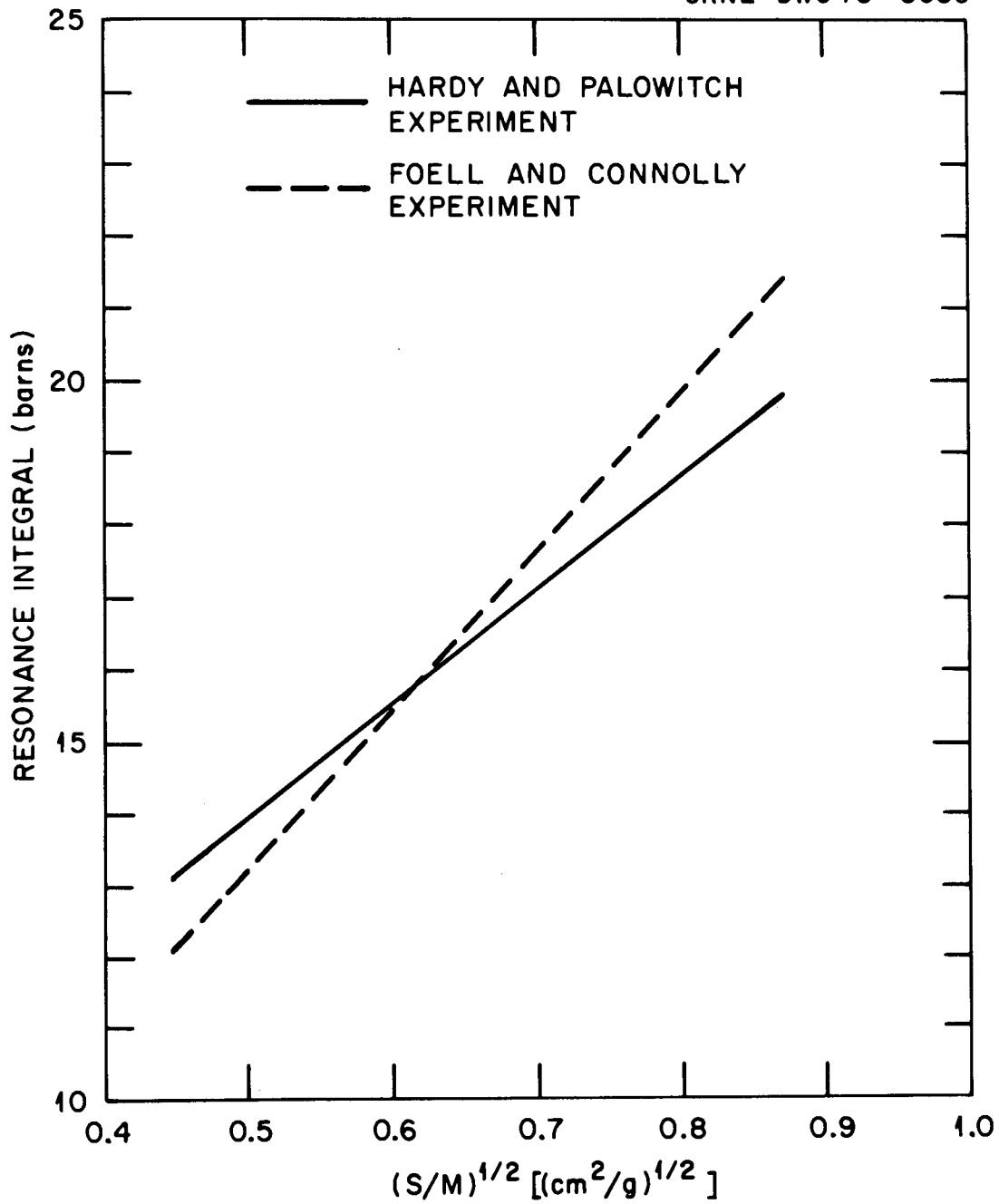


Fig. 4.6. ^{232}Th Resonance Integral ThO_2 Fuel (300°K) (Case 2).

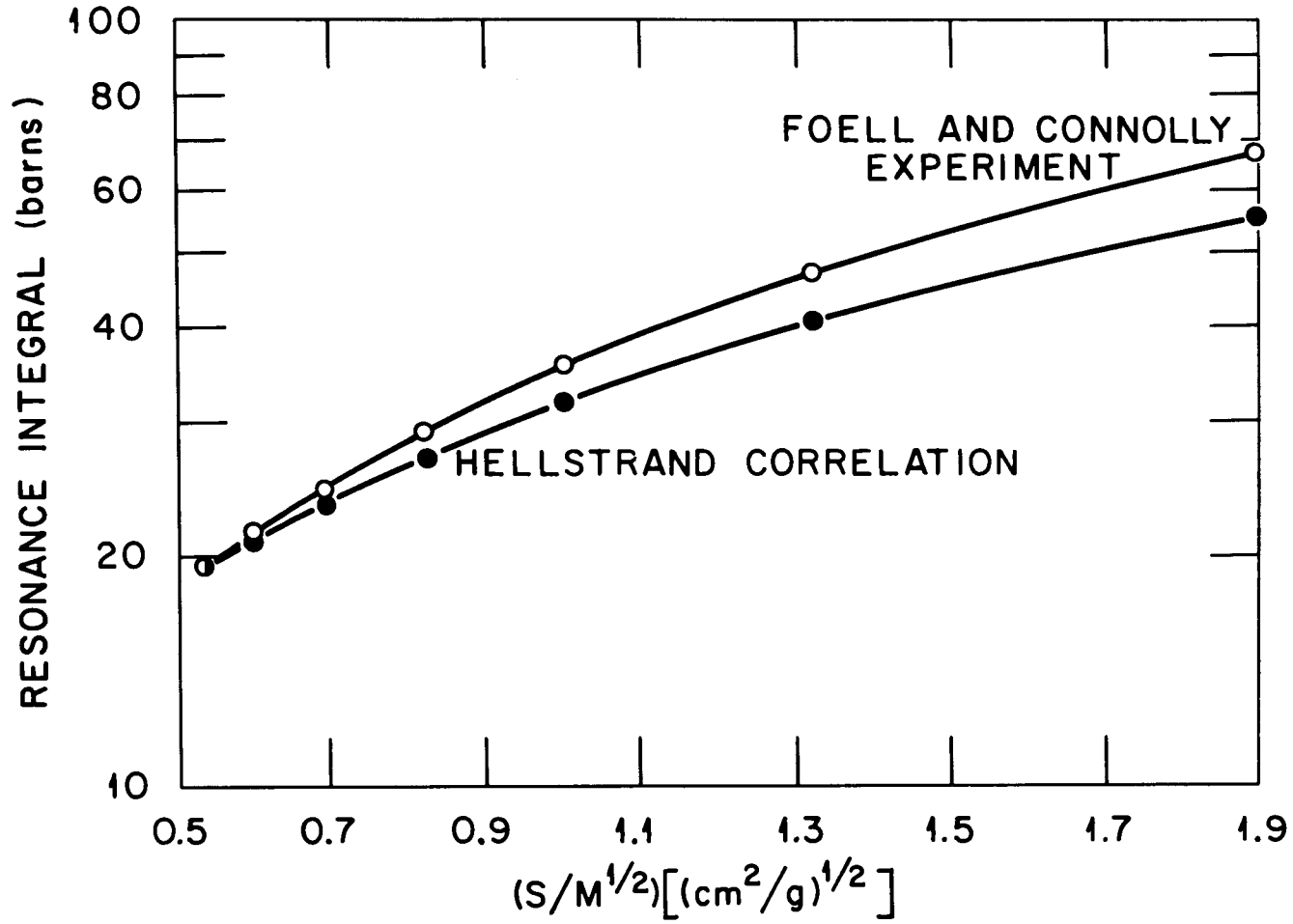


Fig. 4.7. Resonance Integral for ^{238}U in UO_2 (300°K) (Case 1)

5.0 CONCLUSIONS AND RECOMMENDATIONS

The results of the Case 1 UO₂ study indicate that the method used to calculate resonance integrals is reliable to the extent that it is consistent with the Hellstrand correlation for isolated UO₂ rods. Moreover, the ²³⁸U ENDF/B-IV capture data appears to adequately predict the self-shielded integrals, although detailed calculations of additional resonance integral experiments would be desirable. In addition, results obtained using ENDF/B-V data would also be useful, using the isolated rod calculations as a data testing tool.

The Case 2 ²³²Th results indicate a discrepancy of roughly a 6% underprediction of thorium self-shielded resonance integrals. Although preliminary ENDF/B-V evaluations predict a moderate decrease in the infinitely dilute capture integral, it is not clear at this time what effect the version V data will have on shielded systems, although the inferences cited by Ullo suggest that it is possible that version IV data could be responsible for an underprediction of self-shielded thorium resonance integrals. A recalculation of thorium oxide rods using ENDF/B version V and a group structure especially tailored to accommodate both ²³⁸U and ²³²Th resonances is an obvious recommendation.

Finally, for the Case 3 denatured systems, the results of the calculations indicate that the calculated values lie between probable upper and lower bounds, but the accuracy of the calculations cannot be adequately determined for lack of exact experimental data. Again, a consistent benchmark experiment for denatured urania/thoria systems would be desirable or, alternatively, a recalculation of mixed systems containing lead oxide in proportions equal to those of the Foell and Connolly experiment.

ACKNOWLEDGMENTS

The authors wish to thank John Cleveland, Engineering Technology Division, and C. R. Weisbin, Engineering Physics Division, for their interest in the subject of resonance integrals for denatured UO₂/ThO₂ systems and for providing reference data for the systems analyzed. Also, thanks to R. L. Childs, Computer Sciences Division, who provided suggestions and insight into the calculational methodology used in the study. Finally, thanks to C. V. Oldham for her patience in the preparation and typing of this report.

This work was performed for the Engineering Physics Division, Oak Ridge National Laboratory.

REFERENCES

1. L. W. Nordheim, "The Theory of Resonance Absorption," *Proc. Symp. Appl. Math.*, 11 (1961). Providence, RI: American Mathematical Society.
2. F. T. Adler, G. W. Hinman and L. W. Nordheim, "The Quantitative Evaluation of Resonance Integrals," *Proc. 2nd Intern. Conf. Peaceful Uses Atomic Energy, P/1988*, 155-161 (1958).
3. A. J. Goodjohn and G. C. Pomraning, "Reactor Physics in the Resonance and Thermal Regions," *Proc. Nat. Top. ANS* (1966).
4. B. I. Spinrad, J. Chernick and N. Corngold, "Resonance Capture in Uranium and Thorium Lumps," *Proc. 2nd Intern. Conf. Peaceful Uses Atomic Energy, P/1847*, 191-205 (1958).
5. W. Rothenstein, *Collision Probabilities and Resonance Integrals for Lattices*, BNL 563 (T-151) (1959).
6. J. Hardy, Jr., and B. L. Palowitch, "The Effective Resonance Integral and Doppler Coefficient of Thorium-Oxide Rods," *Nucl. Sci. Eng.*, 29, 111-121 (1967).
7. W. K. Foell and T. J. Connolly, "An Investigation of Resonance Absorption in Mixtures of Uranium 238 and Thorium 232," *Nucl. Sci. Eng.*, 26, 399-417 (1966).
8. E. Hellstrand, "Measurements of the Effective Resonance Integral in Uranium Metal and Oxide in Different Geometries," *J. Appl. Physics*, 28, 1493 (1957).
9. E. Hellstrand, P. Blomberg and S. Horner, "The Temperature Coefficient of the Resonance Integral for Uranium Metal and Oxide," *Nucl. Sci. Eng.*, 8, 497-506 (1960).
10. M. Todosow and J. F. Carew, "The Evaluation of Temperature-Dependent Resonance Integrals Using the HAMMER Code," *Trans. Am. Nucl. Soc.*, 27, 915-916 (1977).
11. J. E. Suich and H. C. Honeck, *The HAMMER System*, DP-1064 (1967).
12. R. F. Barry, *LEOPARD - A Spectrum Dependent Non-Spatial Depletion Code for the IBM-7094*, WCAP-3269, 26 (1963).
13. J. R. Lamarsh, *Nuclear Reactor Theory*, Addison-Wesley, pp. 234-235 (1966).
14. C. R. Weisbin et al., *MINX: A Multigroup Interpretation of Nuclear X-sections from ENDF/B*, LA-6486-MS (1976).
15. R. Q. Wright, *A Users Manual for the ORNL Version of SPHINX* (to be published).
16. N. M. Greene, J. L. Lucius, W. E. Ford, III, J. E. White, R. Q. Wright and L. M. Petrie, *AMPX: A Modular Code System for Generating Coupled Multigroup Neutron-Gamma Libraries from ENDF/B*, ORNL/TM-3706 (1976).
17. E. T. Tomlinson, G. de Saussure and C. R. Weisbin, *Sensitivity Analysis of TRX-2 Lattice Parameters with Emphasis on Epithermal ²³⁸U Capture*, EPRI report NP-346 (1977).

18. W. W. Engle, Jr., *A User's Manual for ANISN, A One-Dimensional Discrete Ordinates Transport Code with Anisotropic Scattering*, K-1693 (1967).
19. G. C. Haynes, *AXMIX - ANISN Cross-Section Code*, RSIC PSR-75 (1976).
20. J. Ullo, J. Hardy and N. M. Steen, "Review of Thorium-²³⁸U Cycle Thermal Reactor Benchmark Studies," (to be published in the proceedings of the Thermal Data Testing Seminar, May 22-24, 1978).

Appendix A

MULTIGROUP FORM FOR THE RESONANCE INTEGRAL

Lamarsh gives a physical interpretation to the resonance integral:

. . . the resonance integral is equal to the integral of the absorption cross section over the resonance region which is necessary to account for the observed neutron absorption rate in a flux equal to that existing in the absence of the resonances.

If we assume that an effective absorption cross section, $\sigma_{\text{eff}}(u)$, and a flux (per unit lethargy) $\phi_m(u)$ in the moderator which is equal to that in the fuel in the absence of resonances will give rise to the same number of absorptions due to a cross section $\sigma_a(u)$ and flux $\phi_f(u)$ in the fuel in the presence of resonances, we can write

$$\int_{\text{Res}} \sigma_a(u) \bar{\phi}_f(u) du = \int_{\text{Res}} \sigma_{\text{eff}}(u) \bar{\phi}_m(u) du \quad (\text{A.1})$$

where ϕ denotes a spatial average flux.

Since $\phi_m(u)$ is the flux in the moderator, we will assume that it has attained some asymptotic value, ϕ_{as} , with a $1/E$ behavior. Thus $\phi(u)$ becomes ϕ_{as} , and Eq. (A.1) becomes

$$\frac{1}{\phi_{\text{as}}} \int_{\text{Res}} \sigma_a(u) \bar{\phi}(u) du = \int_{\text{Res}} \sigma_{\text{eff}}(u) du \equiv I \quad (\text{A.2})$$

The right-hand side of Eq. (A.2) is indeed the Lamarsh definition of the resonance integral.

We now define the average value of the flux over the spatial variable as

$$\bar{\phi}(u) = \frac{\int_{\text{vol}} \bar{\phi}(\bar{\mathbf{r}}, u) d^3\bar{\mathbf{r}}}{\int d^3\bar{\mathbf{r}}} = \frac{1}{V} \int_{\text{vol}} \bar{\phi}(\bar{\mathbf{r}}, u) d^3\bar{\mathbf{r}} \quad (\text{A.3})$$

where V is the volume of the fuel or moderator over which the integral is taken. Equation (A.2) can then be written

$$I = \frac{V_{\text{mod}}}{V_{\text{fuel}}} \left[\frac{\int_{\text{res}} du \int_{\text{fuel}} \sigma_a(\bar{r}, u) \phi(\bar{r}, u) d^3\bar{r}}{\int_{\text{mod}} \phi_{\text{as}}(\bar{r}) d^3\bar{r}} \right] . \quad (\text{A.4})$$

We shall now change the variable of integration to energy rather than lethargy. Recall that

$$u = \ln \frac{E}{E_0} ,$$

$$du = \frac{1}{E} dE , \text{ and}$$

$$\phi(u) = E\phi(E) .$$

Thus the integral in the numerator in Eq. (A.4) becomes

$$\int_{\text{Res}} dE \int_{\text{fuel}} \sigma_a(\bar{r}, E) \phi(\bar{r}, E) d^3\bar{r} . \quad (\text{A.5})$$

To transform ϕ_{as} to energy variables, we recall the assumption that ϕ_{as} is not a function of lethargy. Thus

$$\phi_{\text{as}}(u) = \text{const} = E\phi(E) . \quad (\text{A.6})$$

Multiplying both sides by du gives

$$\phi_{as} du = E\phi(E)du = E\phi(E)\frac{1}{E}dE \quad . \quad (A.7)$$

Integrating Eq. (A.7) gives

$$\phi_{as} \int du = \int \phi(E) dE$$

or

$$\phi_{as}(\bar{r}) = \frac{\int \phi(\bar{r}, E) dE}{\int \frac{1}{E} dE} \quad . \quad (A.8)$$

To apply limits of integration to Eq. (A.8), we desire energy limits over which the flux does indeed behave as $1/E$, our original assumption. We now write

$$\phi_{as}(\bar{r}) = \frac{\int_{E_c}^{E_s} \phi(\bar{r}, E) dE}{\int_{E_c}^{E_s} \frac{1}{E} dE} \quad (A.9)$$

where E_s is the maximum energy of source neutrons, and E_c is some thermal cutoff energy below which there are no resonances. Substituting Eqs. (A.9) and (A.5) into Eq. (A.4) gives

$$I = \frac{V_{\text{mod}}}{V_{\text{fuel}}} \left[\frac{\int_{E_c}^{E_s} dE \int_{\text{fuel}} \sigma_a(\bar{r}, E) \phi(\bar{r}, E) d^3\bar{r}}{\int_{\text{mod}} d^3\bar{r} \int_{E_c}^{E_s} \phi(\bar{r}, E) dE / \int_{E_c}^{E_s} \frac{1}{E} dE} \right] \quad (\text{A.10})$$

Putting Eq. (A.10) into multigroup form gives

$$I = \frac{V_{\text{mod}}}{V_{\text{fuel}}} \left[\frac{\sum_g \sum_i V_i \sigma_{a,i,g} \phi_{i,g}}{\sum_{g'} \sum_j V_j \phi_{j,g'} \frac{1}{\Delta U}} \right] \quad (\text{A.11})$$

where g denotes energy groups such that $E_c \leq E_g \leq E_s$, g' such that $E_r \leq E_{g'} \leq E_s$, i and j are spatial intervals in the fuel and moderator, respectively, and ΔU is the total lethargy width spanned by $E_c \leq E_{g'} \leq E_s$.

Appendix B

SUBTRACTING OFF THE THERMAL CONTRIBUTION TO ABSORPTION

In the calculation of resonance absorption to cutoff energy E_1 , it is important not to include absorptions below E_1 . If E_1 is not at the boundary of one of the groups but is below group i so that

$$E_1 < E_{i+1}$$

where E_{i+1} is the lower energy of group i , then the absorptions below group i but above E_1 can be calculated in the following way.

Assume (1) the flux per unit energy varies as $1/E$, and (2) the absorption cross section varies as $1/v$. Then the absorptions A_1 below group i but above E_1 may be written

$$\begin{aligned}
 A_1 &= \int_{E_1}^{E_{i+1}} dE \phi(E) \sigma_a(E) \\
 &= \int_{u_{i+1}}^{u_1} du \phi(u) \sigma_a^0 \frac{v_0}{v} \\
 &= \phi_u \sigma_a^0 \int_{u_{i+1}}^{u_1} du e^{-\frac{1}{2}(u_0 - u)} \\
 &= \phi_u \sigma_a^0 e^{-\frac{1}{2}u_0} 2 \left(e^{-\frac{1}{2}u_1} - e^{-\frac{1}{2}u_{i+1}} \right) \\
 &= 2 \phi_u \sigma_a^0 v_0 \left(\frac{1}{v_1} - \frac{1}{v_{i+1}} \right) . \tag{B.1}
 \end{aligned}$$

This last expression may be related to the group flux ϕ_i and written as follows

$$A_1 = 2 \phi_i \sigma_a^0 v_0 \left(\frac{1}{v_1} - \frac{1}{v_{i+1}} \right) / \frac{1}{\Delta u_i} \quad (B.2)$$

In this expression, the cross section is normalized to a standard value σ_a^0 at velocity v_0 . It might be preferable to relate to the total absorptions A_i in group i . Under the assumptions this is

$$A_1 = 2 \phi_i \sigma_a^0 v_0 \left(\frac{1}{v_{i+1}} - \frac{1}{v_i} \right) / \frac{1}{\Delta u_i} \quad (B.3)$$

Hence, combining the expressions for A_i and A_1 we have

$$A_1 = A_i \left(\frac{1}{v_1} - \frac{1}{v_{i+1}} \right) / \left(\frac{1}{v_{i+1}} - \frac{1}{v_i} \right) \quad (B.4)$$

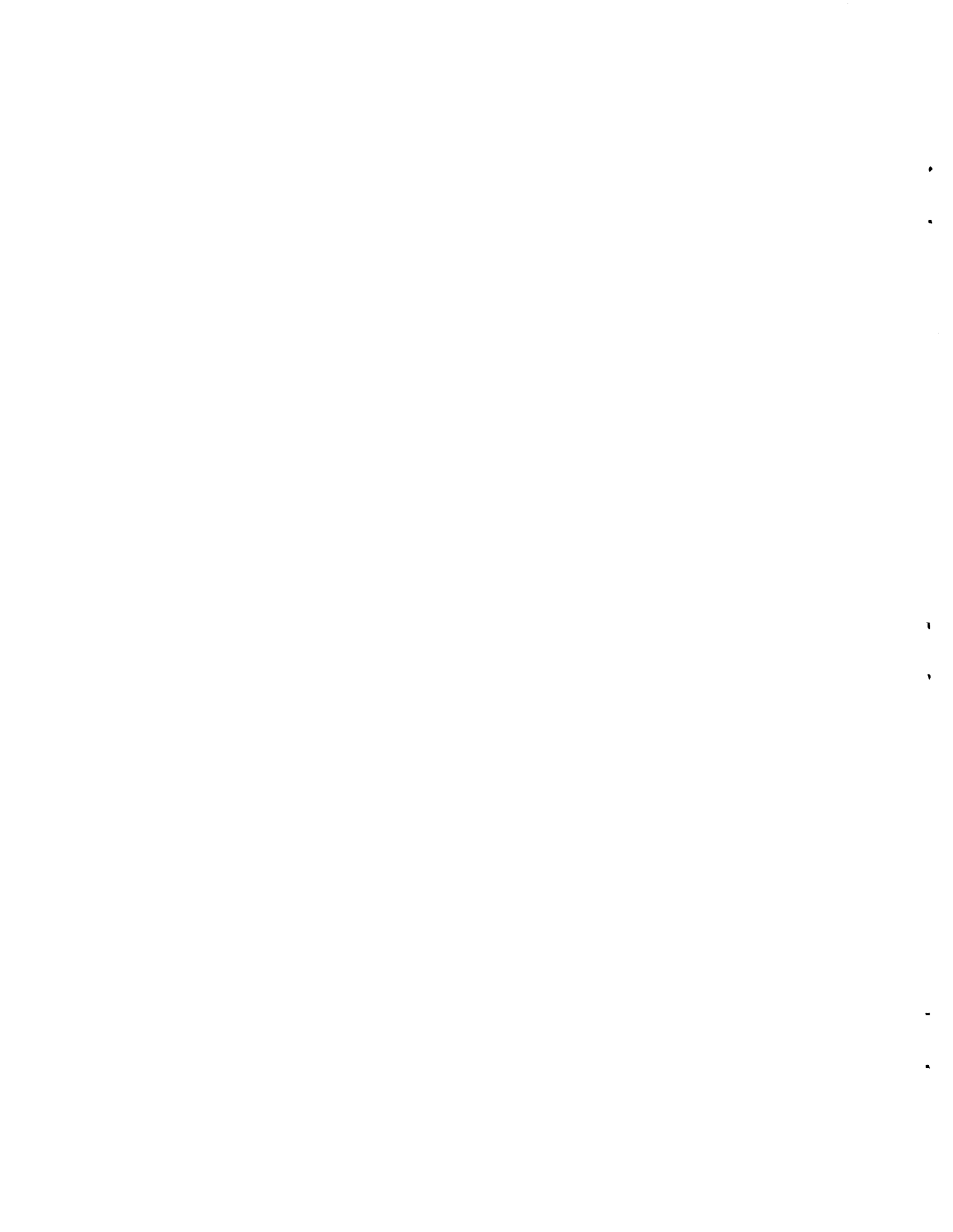
or

$$A_1 = A_i \left(\frac{v_i}{v_1} \right) \left(\frac{v_{i+1} - v_1}{v_i - v_{i+1}} \right) = A_i \cdot \frac{E_i + (E_i E_{i+1})^{1/2}}{E_1 + (E_1 E_{i+1})^{1/2}} \cdot \frac{E_{i+1} - E_1}{E_i - E_{i+1}} \quad (B.5)$$

where A_1 is the absorptions below group i but above energy E_1 corresponding to speed v_1 , and A_i is the absorption in group i with upper velocity bound v_i and lower velocity bound v_{i+1} and with corresponding energy bounds E_i and E_{i+1} .

Appendix C

FORTRAN PROGRAM TO CALCULATE MULTIGROUP FIXED SOURCES



```

C*****PROGRAM TO CALCULATE MULTIGROUP SOURCES FOR RESONANCE
C*****INTEGRAL CALCULATION
C
      DIMENSION XSEC(136,17),FLUX(130),SRC(130)
      DATA L1,L2/4H 15R,4H0.0 /
C*****READS LEHPAGY WIDTHS FROM CARD INPUT
      READ(5,100) (FLUX(I),I=1,130)
100  FORMAT(6E12.5)
C*****READS MULTIGROUP CROSS SECTIONS FROM 'GID' TAPE ON UNIT 1.
C*****MODERATOR (WATER) CORRESPONDS TO MATERIAL NUMBER 17 ON GID TAPE
      READ(1) XSEC
C*****COMPUTES MULTIGROUP SOURCE FOR GROUP ONE. NO DOWNSCATTER INTO
C*****GROUP ONE.
      SRC(1)=(XSEC(5,17)-XSEC(6,17))*FLUX(1)
C*****BEGINNS SOURCE CALCULATION LOOP FOR REMAINING GROUPS
      DO 1 IG=2,130
      READ(1) XSEC
      SCAT=0.0
C*****COMPUTES 'REMOVAL' CROSS SECTION
      SIGP=XSEC(5,17)-XSEC(6,17)
      II=IG-1
      DO 5 NE=1,II
C*****COMPUTES SCATTERING INTEGRAL FOR GROUP IG.
      SCAT=SCAT+FLUX(IG-NE)*XSEC(II+6,17)
5      CONTINUE
C*****COMPUTES SOURCE FOR GROUP IG FROM NEUTRON BALANCE FOR
C*****INFINITE MEDIUM WITH NO UPSCATTER OR FISSION.
      SRC(IG)=SIGP*FLUX(IG)-SCAT
1      CONTINUE
      DO 15 IG=1,130
C*****PUNCHES GROUPWISE SOURCES IN 'FIDO' FORMAT FOR USE IN
C*****ANISN SOURCE INPUT ARRAY
      WRITE(7,20) L1,L2,L1,SRC(IG)
C*****PRINTS GROUPWISE SOURCES IN FIDO FORMAT
      WRITE(6,21) L1,L2,L1,SRC(IG)
20  FORMAT(2A4,1X,1A4,E12.5)
21  FORMAT(1H ,2A4,1X,1A4,F12.5)
15  CONTINUE
      STOP
      END

```

```

HASP-11 JOB STATISTICS -- 42 CARDS READ -- 0 LINES PRINTED --

```



INTERNAL DISTRIBUTION

- | | | | |
|--------|---|--------|------------------------------------|
| 1. | L. S. Abbott | 30. | J. S. Tang |
| 2-6. | V. C. Baker | 31. | J. E. Vath |
| 7. | J. Barhen | 32. | D. R. Vondy |
| 8. | M. A. Bjerke | 33. | C. R. Weisbin |
| 9. | H. P. Carter/A. A. Brooks/
CSD Library | 34. | R. M. Westfall |
| 10. | R. L. Childs | 35. | G. E. Whitesides |
| 11-15. | J. C. Cleveland | 36. | M. L. Williams |
| 16. | G. de Saussure | 37. | R. Q. Wright |
| 17. | H. L. Dodds, Jr. | 38. | A. Zucker |
| 18. | W. E. Ford, III | 39. | P. Greebler (consultant) |
| 19. | N. M. Greene | 40. | W. B. Loewenstein (consultant) |
| 20. | F. C. Maienschein | 41. | R. Wilson (consultant) |
| 21-25. | J. H. Marable | 42-43. | Central Research Library |
| 26. | J. W. McAdoo | 44. | Y-12 Document Reference
Section |
| 27. | J. V. Pace, III | 45-47. | Laboratory Records |
| 28. | L. M. Petrie | 48. | Laboratory Records - RC |
| 29. | R. W. Roussin | 49. | ORNL Patent Section |
| | | 50. | EPD Reports Office |

EXTERNAL DISTRIBUTION

51. H. Goldstein, Division of Nuclear Science and Engineering, Columbia University, 520 W. 120th Street, New York, New York 10027
52. J. N. Rogers, Division 8324, Sandia Laboratories, Livermore, California 94550
53. Chief, Mathematics and Geoscience Branch, Department of Energy, Washington, DC 20545
54. Office of Assistant Manager for Energy Research and Development, Department of Energy, Oak Ridge Operations, Oak Ridge, Tennessee 37830
- 55-81. Technical Information Center, Department of Energy, Oak Ridge, Tennessee 37830